Atomic structure of the Ag(001) $c(2\times2)$ Mn surface alloy

P. Schieffer,* C. Krembel, M.-C. Hanf, and G. Gewinner
Laboratoire de Physique et de Spectroscopie Electronique (UMR-CNRS 7014), Faculté des Sciences et Techniques, 4 rue des Frères Lumière, F-68093 Mulhouse Cedex, France

Y. Gauthier
Laboratoire de Cristallographie CNRS, Boîte Postale 166, F-38042 Grenoble Cedex, France
(Received 7 December 2001; revised manuscript received 12 February 2002; published 13 June 2002)

The structure of the unstable $c(2\times2)$ Mn surface alloy that is formed on Ag(001) upon deposition of an Mn monolayer at room temperature is determined by low-energy electron diffraction (LEED). The optimized structure model is basically a two-monolayer-thick Mn_xAg_{100-x} alloy that is ordered in a checkerboard arrangement in the first layer and random in the second layer, with substantial deviations from ideal order and stoichiometry $x=50$. The surface alloy essentially prolongs the face-centered-cubic Ag lattice, with interlayer distances $d_{12}=1.985\pm0.010$ Å and $d_{23}=2.030\pm0.008$ Å only slightly reduced with respect to Ag bulk, and a buckling of 0.07 Å (Mn displaced outwards) in the top layer. The present work clearly confirms the unusually large atomic volume of Mn in this environment as found in previous surface-extended x-ray absorption fine structure work [P. Schieffer, M.-H. Tuilier, M.-C. Hanf, C. Krembel, G. Gewinner, D. Chandesris, and H. Magnan, Phys. Rev. B **57**, 15 507 (1998)] and disproves the geometry inferred from an earlier LEED study [Wondong Kim, Wookje Kim, S.-J. Oh, J. Seo, J.-S. Kim, H.-G. Min, and S.-C. Hon, Phys. Rev. B **57**, 8823 (1998)].

DOI: 10.1103/PhysRevB.65.235427 PACS number(s): 68.55.−a, 61.14.Hg, 68.47.De

I. INTRODUCTION

The properties of Mn-based surface alloys have recently attracted considerable attention because of the large magnetic moment expected due to a half-filled $3d$ shell. For Mn/Ni(001) (Ref. 1) and Mn/Pd(001) (Ref. 2), the alloy may be several atomic layers thick and ordering takes place within the whole film. In contrast, a true one-monolayer-thick (1-ML-thick) surface alloy is formed after evaporation of 0.5 ML of Mn on Co(001) at room temperature (RT) (Ref. 3) or on Ni(001) and Cu(001) above 270 K.[4,5] For Mn/Cu(001), quantitative low-energy electron diffraction (LEED) analysis reveals that in the topmost plane each Mn atom is surrounded by four Cu atoms and that the alloy presents an unusually large corrugation, with the Mn atoms lying 0.30 ± 0.02 Å higher than the Cu atoms.[4,6]

Now when Mn is deposited on Ag(001) at RT, a $c(2\times2)$ superstructure is obtained as well for coverages ranging from 0.5 to 4 ML, and the brightest half-order spots are observed for 1–1.5 ML.[7] At 1 ML, according to x-ray photoelectron diffraction[8] and surface-extended x-ray absorption fine structure[9] (SEXAFS) studies, Mn atoms are essentially confined within the surface and subsurface planes, and the Mn-Ag bilayer alloy is generally inhomogeneous, in the sense that the surface contains $c(2\times2)$ and $p(1\times1)$ domains simultaneously. According to the best-fit SEXAFS model, in the $c(2\times2)$ areas, the topmost plane exhibits about 50% Mn and 50% Ag atoms ordered in a checkerboard arrangement, and the subsurface sites are rather occupied randomly by Ag and Mn atoms. In contrast, the (1×1) domains display a pure Ag surface above an Mn-rich plane, i.e., an inverted Mn monolayer structure. The Mn-Ag interatomic distance is about 2.86 Å as compared to 2.89 Å for the Ag-Ag distance in bulk, which suggests a surprisingly weak interlayer distance contraction. This disagrees with a previous LEED study, where the Mn-Ag alloy is described in terms of a bilayer-ordered surface alloy, with the Mn and Ag atoms ordered in a checkerboard arrangement within the two first atomic planes and a very large contraction of 8.3% of the interlayer distance between second and third atomic planes.[10]

Actually, this discrepancy can be related to the question of the stability of the films. Indeed, the film obtained after deposition of 1 ML of Mn at RT is not stable at RT, as Mn adatoms tend to change place spontaneously with Ag atoms from the substrate. This exchange mechanism takes place during and after Mn deposition and slows down within a few hours once the subsurface plane becomes Mn saturated.[7,11] This means that LEED measurements have to be performed only on a film whose atomic structure has been frozen by cooling, as atomic exchange and diffusion are thermally activated phenomena. Whereas in the SEXAFS work[9] the structure was indeed stabilized by cooling at 100 K, LEED data in Ref. 10 have been recorded at RT, that is, on an unstable film, which means that the results are questionable.

For all these reasons, it was desirable to achieve a new LEED investigation on a frozen and carefully optimized Mn-Ag surface alloy involving 1 ML Mn. We definitely show that the topmost plane of the alloy is made of $c(2\times2)$ domains where every Mn atom is surrounded by four Ag atoms, while within the second atomic plane the Mn and Ag are located at random. Deviations from ideal structure are present, mainly related to antiphase boundaries between small adjacent $c(2\times2)$ domains. The atoms occupy fcc Ag lattice sites, and the first and second interlayer distances are contracted by 3% and 0.7%, respectively, with respect to bulk Ag, in nice agreement with earlier SEXAFS work.[9]

II. EXPERIMENT

The experiments were performed in a UHV chamber with a base pressure below 2×10^{-10} mbar. The Ag(001) single-crystal surface was prepared by standards methods.[7] A nominal monolayer of Mn [1 ML is defined with respect to the Ag(001) surface atomic density] was deposited onto clean Ag(001) kept at 210 K; afterwards, the sample was slowly ramped to 298 K (RT) upon monitoring the intensity of the $c(2\times2)$ superstructure spots. As soon as the latter reached a maximum, the film was quickly cooled down to ~100 K for the LEED measurements, as at liquid-nitrogen temperature the films are found to be quite stable with the additional benefit of lower thermal disorder. This preparation method gave better LEED diagrams than a simple Mn deposition at RT and subsequent cooling at 100 K, and the relevant structure appears to be fairly homogeneous with only a small amount ($\leqslant$10%) of reordering towards an inverted Mn monolayer. Further details on sample preparation and characterization can be found in Ref. 7.

Conventional LEED optics consisting of four grids and a fluorescent screen has been employed. The LEED spot intensities versus incident electron energy, $I(E)$, have been extracted from pictures taken with a charge-coupled device (CCD) camera and using the method described in Ref. 12. The data set includes nine inequivalent beams (six integer and three fractional beams) corresponding to a cumulated energy range of 1511 V (1003 and 508 V, respectively, for integer and fractional beams).

III. LEED CALCULATIONS

LEED calculations were conducted in a similar manner as in our previous study of the $c(2\times2)$ Mn antiferromagnetic overlayer[12] and of the inverted Mn layer on Ag(001).[13] We used the code of Moritz, which allows both for a standard grid search and for an automatic fit of the main parameters.[14] The same sets of phase shifts and Debye temperature were used to describe the scattering and effect of temperature. We also started the analysis with the previously optimized values of the inner potential. The optimization was rather straightforward as the periodicity is that of the bulk and the parameters reduce to average concentrations of the first four layers, the corresponding interlayer distances, and finally, the inner potential V_0 and the absorptive potential V_i (both constant with energy) and the Debye temperature. Beforehand, with fewer parameters, we optimized the scattering conditions around the normal to the crystal incidence using the adapted symmetries.

The angles were checked several times in the course of the analysis and the actual conditions read $(\vartheta,\Phi)=(1.25°,28°)$.

The agreement was assessed by the metric distance D_1 (Ref. 15) [$=R_{de}/2$ (Ref. 14)] and by Pendry's r factor R_p (Ref. 16) for comparisons. The error bars follow from the variance of R_p:

$$\mathrm{Var}(D_1)=R_{p\,\min}\times(8V_i/\Delta E)^{1/2}$$
$$=0.197\times(8\times4.5/1511)^{1/2}=0.03,$$

where ΔE is the total energy range entering the calculation.

In order to take into account chemical ordering, we distinguished two inequivalent sites in the unit cell corresponding to the checkerboard arrangement, within the first and third atomic planes. Indeed, from symmetry arguments one site only exists in layer 2. However, in Ref. 10, the authors have considered both sites in the unit cell for the surface and subsurface planes, a situation that actually implies 2-mm rather than 4-mm point group symmetry and rotationally equivalent domains. We will come back to this point later. The composition of each site was determined by means of the average-t-matrix approximation[17,18] (ATA) in the first three layers. Both species were assumed to occupy the nodes of the fcc net at random. In the following, the atoms of the outer layers were supposed to occupy the bulk Ag(001) position except for the interlayer distances that were allowed to vary.

For V_0 and V_i, the optimum occurs at -6 and 4.5 eV, respectively, values almost identical to those found for a previous work.[12] The Debye temperature was checked punctually in the top two layers: the optimum was reached for 157 K in layer 1 and 288 K for layer 2, while the Ag substrate was assigned a value of 250 K.

A maximum of ten phase shifts at the highest energy (385 eV) was used in the calculation, in contrast with the study of Kim *et al.* who limited this parameter to 7.[10] The latter number may be insufficient even at 160 eV (their highest energy is actually 280 eV) where Mn and Ag partial scattering amplitudes t_l for $l\geqslant6$ have still large values ($t_7=0.11$, $t_8=0.05$,...).

IV. RESULTS: COMPOSITION AND STRUCTURAL MODEL

The results are summarized in Table I, and the r-factor evolutions versus structural parameters are presented in Figs. 1–5. Near-optimum rather than exactly optimum parameters explain the small changes in the minimum r factor in the different figures. The errors bars are derived from the variance of R_p and again are presented for near-optimum values. Figure 1 shows that the first interlayer spacing is contracted by 3% with respect to the bulk spacing (2.044 Å): the next one is still reduced by 0.7%, and there is an extremely weak expansion, 0.6%, below. As can be seen in Fig. 2, the mixed top layer is clearly corrugated, the Mn-rich site being 0.07 Å above the Ag-rich sublayer (Fig. 2). Hence the actual interlayer spacing from the first to the second layer, with respect to the center-of-mass plane, is about 2.01 Å. We also tried to move out of plane half of the atoms of layer 3, but within the sensitivity of the method, the best agreement results from coplanar atoms.

The evolution of the r factors versus layer composition, shown in Figs. 3–5 for layers 1, 2, and 3, respectively, clearly demonstrates a strong tendency to $c(2\times2)$ chemical order restricted to the topmost layer.

In terms of average concentrations, the top three layers contain, respectively, $\langle C_1\rangle=43\%$, $\langle C_2\rangle=34\%$, and $\langle C_3\rangle=4\%$ Mn. This corresponds to a monotonous decrease of the adatom concentration with depth (Figs. 3–5), in contrast

TABLE I. Optimum parameters for the surface Mn-Ag alloy on Ag(001). Here C_{ij} is the atomic fraction of Mn on site j in layer i; d_{ij} is the vertical spacing between the lowest atom in layer i and the highest atom in layer j. Also Z_{11} is the buckling in layer 1; in the present instance, Mn atoms lie above the Ag sublattice. The last two lines show the equivalent parameters for the Mn films—surface antiferromagnetic layer with $c(2\times2)$ periodicity (Ref. 12) and the inverted (1×1) Mn layer (Ref. 13).

Structure	D_1	R_p (Å)	d_{12} (Å)	d_{23} (Å)	d_{34} (Å)	Z_{11} (Å)	C_{11} (% Mn)	C_{12} (% Mn)	C_{21}[a] (% Mn)	C_{31} (% Mn)	C_{32} (% Mn)
Surf. alloy	0.120	0.197	1.985	2.030	2.057	.07	9	78	34	7	2.5
Layer average							43		34	4.5	
Error bars			±0.010	±0.008	±0.016	±0.015	±12	±17	±13	±10	±12
Surf. alloy LEED[b]		0.267	2.036	1.873		0.03	0	100	0/100*,[a]	0	0
Total energ calc.[b]			1.789	1.989		−0.027					
Inverted Mn layer[c]	0.142	0.248	1.974	1.974	2.035		8		90	10	
Mn overlayer[d]	0.153	0.311	2.00	2.029	2.04		85		0–10	0	

[a]From symmetry arguments one site exists in layer 2; Kim *et al.*, however, have distinguished both sites in the unit cell (see text).
[b]Reference 10.
[c]Reference 13.
[d]Reference 12.

with many bimetallic alloys where, instead, the concentration shows damped oscillations.[18]

None of the sites, whether in the first or third layer, is actually occupied by a single species. In layer 1, one site contains a random mixture of 9% Mn and 91% Ag, the other being Mn rich (78%) (Fig. 3). The total amount of Mn is not sufficient to allow a perfect alloy to develop all over the surface, although the final state is close to $Mn_{50}Ag_{50}$ in layer 1. The $c(2\times2)$ domains have grown and have reached their maximum size, but the order does not develop over very long distances, which would yield clear-cut concentrations on the surface sites at least. Locally, the checkerboard arrangement is present, each domain being separated from surrounding ones by antiphase boundaries. During the short RT anneal of the Mn deposit, the exchange of atoms (Mn versus Ag) between layers competes with surface diffusion, leading to this limited ordering. It is the presence of these antiphase boundaries which explains the apparent partial ''random'' distributions of Mn and Ag species in layer 1 in LEED calculations, Ag atoms occupying the positions of Mn in the next domain and vice versa, not accounting for other kinds of defects. Yet only small (1×1) pure Ag domains might be present, as indicated by a previous study.[7] The presence of a large number of small $c(2\times2)$ antiphase domains is quite consistent with the observed width of the LEED reflections: super-

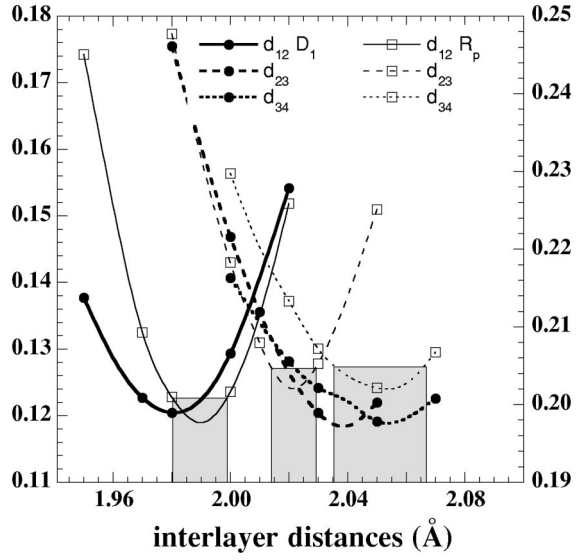

FIG. 1. *r*-factor variations with the interlayer distances. The error bars, derived from the variance of R_p, are shown for near optimum values.

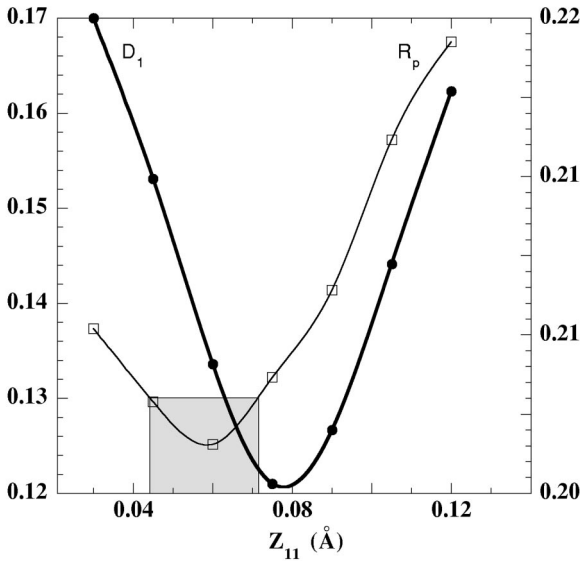

FIG. 2. *r*-factor variations with respect to the buckling (Mn-rich site shifted out) of layer 1 for near-optimum values.

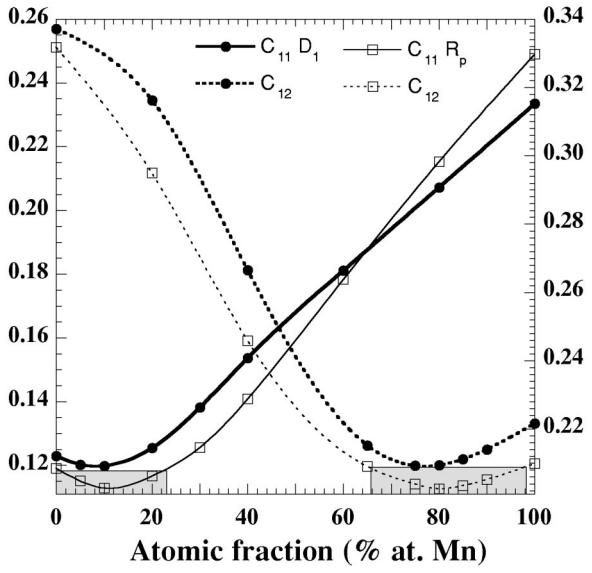

FIG. 3. *r*-factor variations with Mn concentration of both sites in the top layer for near-optimum values.

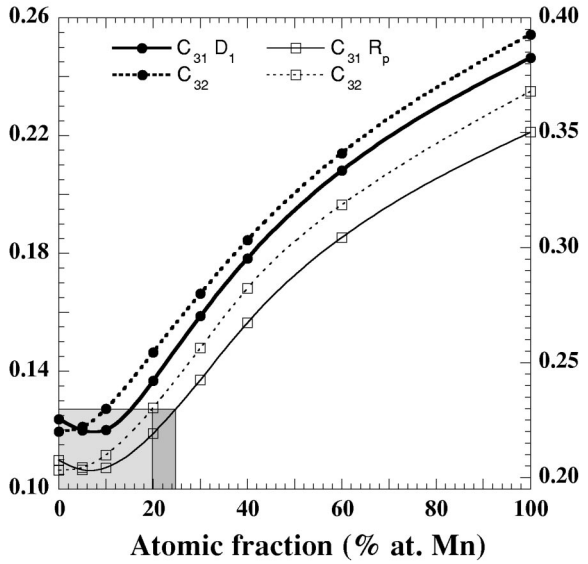

FIG. 5. Same as Fig. 3 for layer 3.

structure spots are definitely broader than integral order ones, as already reported in earlier work,[19] and indicate typical coherent domains sizes of a few lattice parameters only.

V. QUALITY OF THE AGREEMENT

In the present case the agreement is pretty good in comparison with the two previous cases of Mn films where (almost) pure Mn layers alternate with (almost) pure Ag ones (Table I). The metric distance ($D_1 = 0.120$) is quite good if compared with other surface or bulk alloys.[18] Restricting the comparison to Mn films on Ag(001), all *r* factors yield lower values for the present study. R_p is also much lower than the value obtained by Kim *et al.*,[10] giving more confidence in our results. As can be judged from Figs. 1–5, within error bar, all *r* factors yield the same geometry and composition, the largest difference occurring for the buckling, which happens to be a little larger with D_1 (0.075 Å) than for R_p (0.065 Å), and for the second interlayer distance d_{23}. One can judge this correspondence between experimental and calculated spectra in Fig. 6.

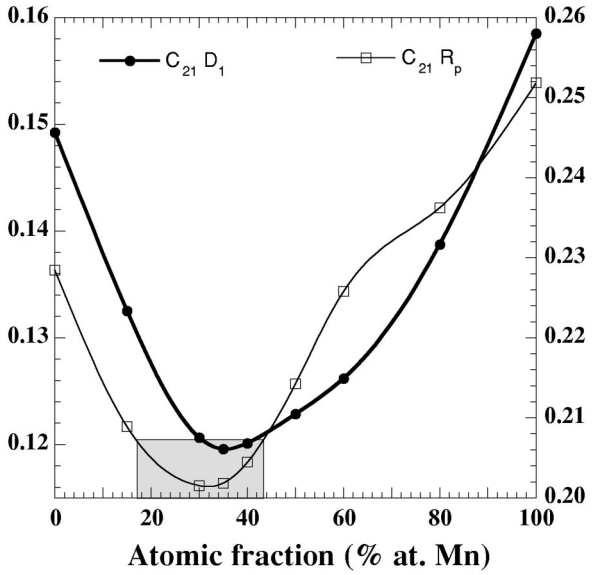

FIG. 4. Same as Fig. 3 for layer 2.

VI. DISCUSSION: COMPARISON WITH PREVIOUS WORKS ON THE SAME STRUCTURE

The present LEED results are in perfect agreement with those obtained from x-ray photoelectron diffraction (XPD) anisotropy and from measurements of the intensity and width of LEED spots as a function of the temperature.[7,9] For this particular structure a 45% Mn+55% Ag content in the top layer is inferred from analysis in Ref. 7, which corresponds within 2% to the present LEED findings. The difference in the second layer is hardly larger since we find 34% Mn for a ~45% estimation from XPD anisotropy. Here too the conclusions from both studies are consistent in the sense that a random distribution of Mn prevails.

In terms of the average composition, this is not far from the LEED results of Kim *et al.*,[10] who end with an alloy extending over two layers. However, the picture is somewhat different in the sense that they arrive at a perfect alloy, with a stoichiometric composition (50% Mn, 50% Ag), while we instead find a short-range ordering in the top layer associated with a random distribution in the layer below.

Regarding the optimum composition of layer 1, if we fix the concentration of both sites to 0 and 100%—the model of Kim *et al.*—the *r* factors increase from $D_1 = 0.120$ and $R_p = 0.197$ to $D_1 = 0.134$ and $R_p = 0.214$, respectively, showing unambiguously that the actual Mn content is lower than in a perfectly ordered layer. Similarly, tests were performed with two inequivalent sites in layer 2. Such a situation implies averaging over two domains so as to account for the lower-

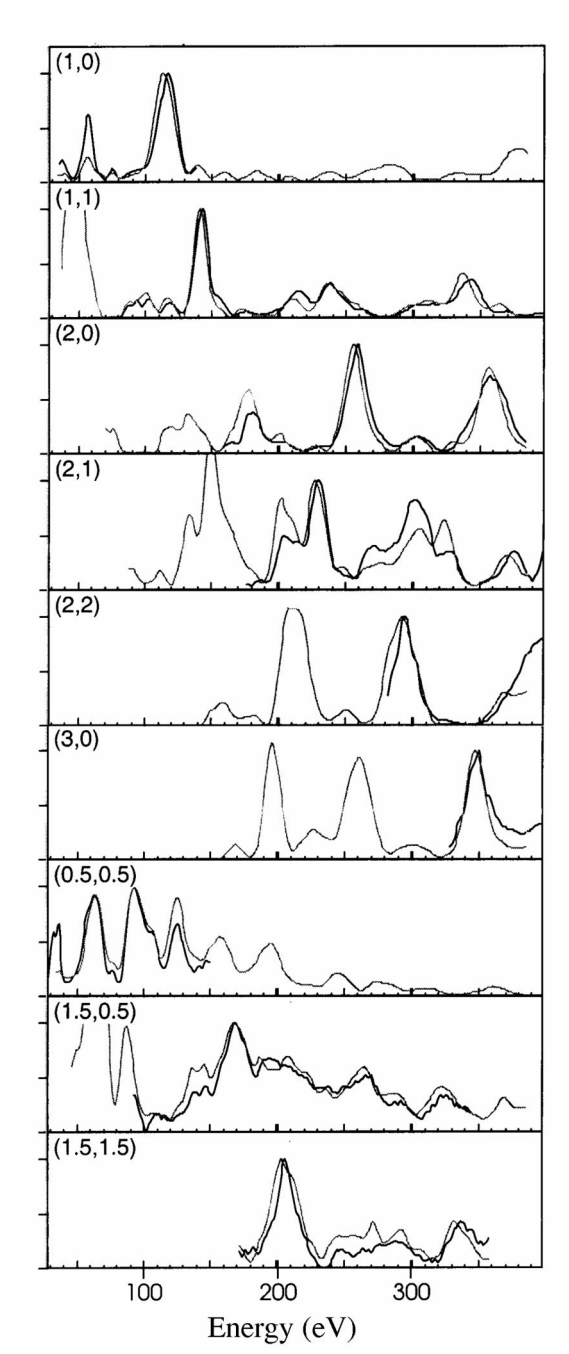

FIG. 6. LEED intensities (in arbitrary units) vs energy (in eV) for the MnAg alloy phase on Ag(001) calculated for near-optimum parameters (thin line) as compared to experiment (thick line).

ing of the symmetry of the slab made of two stoichiometric layers and of the apparent $c(2\times2)$ symmetry of the pattern. The best r factors occur for two sites containing $C_{21}=C_{22}\sim40\%$ Mn—that is, very close to what we obtained considering a single site and random distribution ($C_{21}=34\%$: cf. Table I)—whereas the same r factors increase quite significantly for a stoichiometric and perfectly ordered layer—a pure Mn site associated with a pure Ag site—$D_1=0.145$, $R_p=0.220$. We conclude thus that this stoichiometric bilayer-ordered alloy can be discarded at the expense of a locally ordered layer on top of a truly random $Mn_{34}Ag_{66}$ mixture.

The same assumption—a perfect two-layer-ordered MnAg slab—probably led Kim *et al.* to conclude that, while the first interlayer spacing is bulklike (less than 0.5% contraction compared to 3% in our case), the second spacing d_{23} is contracted by as much as 8.3%, in clear contrast with our finding of an almost bulklike distance. They attribute this strange contraction to the ''insensivity of LEED to the atomic structure of the Ag atoms in the third layer.'' This is a strange claim as, in many studies of either surface or bulk alloys—including the (111) orientation where the interlayer spacing is larger—one could detect the geometry changes and/or composition for such deep layers. To illustrate the point we have plotted the variations of r factors versus the different optimized parameters (Figs. 1–5). While the sensitivity is obviously less marked in the third layer (Fig. 5), it is nevertheless quite sufficient to extract the structure and Mn concentration as well.

Part of the discrepancy obviously arises from differences in the calculations—assumption on the model (ordered or disordered alloy), number of phase shifts, third layer composition included or not, nonstoichiometry of alloy layers—but the experiment (alignment, preparation conditions, total energy range in the data set) itself may have contributed: indeed, as stated in the Introduction, temperature and time are known to influence the composition of the surface layers via diffusion phenomena.[7]

Finally, we wish to focus also on the corrugation of the top layer: here also there is a clear quantitative difference between Ref. 10 and our results (0.03 Å instead of 0.07 Å), whereas both analyses find an Mn sublattice sitting above the Ag sublattice. Concerning the amount of data, it may be remarked that, in the case of Kim *et al.*, only one fractional beam was measured for a relative weight of ~10% in the total energy range (~80 V out of 800 V), while, in our case, $c(2\times2)$ data represent more than 30% (500 V out of 1500 V), which may add to the origin of the difference in the LEED results. With such a ratio and enlarged database, we are more sensitive to the buckling of the surface layer. As there is a strong interdependence of the geometrical parameters, this weak value of the buckling may be correlated to the too small spacing they found for d_{23}. In addition, we note that their total energy calculation results for an interlayer distance fit much better with our results than with those of the authors.

In addition, let us point out the excellent agreement between our best-fit model geometry and previous SEXAFS studies. From this model we derive a mean Mn-Ag distance of 2.87 ± 0.02 Å as compared to 2.86 ± 0.02 Å in Ref. 9.

VII. CONCLUSION

In summary, we have shown that the surface of the AgMn alloy resulting from deposition of 1 ML of Mn on Ag(001) is made of $c(2\times2)$ domains where Mn and Ag atoms are locally ordered in a checkerboard arrangement. The subsurface plane contains $34\pm13\%$ Mn located at random on the fcc sites. The interlayer distances d_{12} and d_{23} are slightly contracted (respectively, 1.985 and 2.030 Å) with respect to bulk

Ag(001), while there is a small corrugation of the Mn atoms (0.07 Å).

Clearly, the MnAg alloy differs substantially from the $c(2\times2)$ surface alloys observed for 0.5 ML of Mn on Cu(001) or Ni(001). Indeed, much more Mn is found within the subsurface plane (34% for 1 ML Mn) than in the case of Cu(001) (12%),[5] and the corrugation within the top layer is lower for MnAg (0.07 Å) than for MnCu (0.3 Å). In addition, the $c(2\times2)$ Mn-Ag alloy correlation length is about a few lattice parameters, whereas for Mn/Cu(001), alloy terraces and islands larger than 100 Å can be found.[5] The larger lattice parameter for Ag (4.09 Å) than for Cu (3.61 Å) has to be taken into account, and the most remarkable point here is the exceptionally large Mn atomic size in the Mn/Ag surface alloy. However, the Mn atomic size for the more stable inverted monolayer (16.40 $Å^3$) is close to that corresponding to the $c(2\times2)$ surface alloy (16.68 $Å^3$) or Mn overlayer (16.70 $Å^3$) and is much larger than in bulk Mn (12.20 $Å^3$), as well as in the MnCu surface alloy (11.69 $Å^3$).[5,12] Hence a similar very large magnetovolume effect is evidenced for the various Mn/Ag(001) systems. X-ray absorption measurements have shown that within the $c(2\times2)$ Mn-Ag alloy the Mn atoms are in a high-spin state, comparable to the inverted monolayer as well as overlayer.[20] Possibly, theoretical work such as the studies of Eder and co-workers,[21] who consider generalized gradient corrections (GGC's) to the exchange correlation functional, might better reproduce the present large magnetovolume effect than the usual local density functional methods, which fail seriously in this respect.

ACKNOWLEDGMENTS

One of us (Y.G.) is indebted to the Institut du Développement et des Ressources en Informatique Scientifique (IDRIS) for his support with computing time. We wish to thank W. Moritz for providing the LEED code used for the present analysis.

*Present address: Laboratoire PALMS, Université de Rennes-1, 35700 Rennes, France.

[1] M. Wuttig and C. C. Knight, Phys. Rev. B **48**, 12 130 (1993).
[2] D. Tian, R. F. Lin, F. Jona, and P. M. Marcus, Solid State Commun. **74**, 1017 (1990).
[3] B.-Ch. Choi, P. J. Bode, and J. A. C. Bland, Phys. Rev. B **58**, 5166 (1998).
[4] T. Flores, M. Hansen, and M. Wuttig, Surf. Sci. **279**, 251 (1992).
[5] M. Wuttig, C. C. Knight, T. Flores, and Y. Gauthier, Surf. Sci. **292**, 189 (1993).
[6] M. Wuttig, Y. Gauthier, and S. Blügel, Phys. Rev. Lett. **70**, 3619 (1993).
[7] P. Schieffer, M.-C. Hanf, C. Krembel, and G. Gewinner, Surf. Sci. **446**, 175 (2000).
[8] P. Schieffer, C. Krembel, M.-C. Hanf, and G. Gewinner, Surf. Sci. **400**, 95 (1998).
[9] P. Schieffer, M.-H. Tuiler, M.-C. Hanf, C. Krembel, G. Gewinner, D. Chandesris, and H. Magnan, Phys. Rev. B **57**, 15 507 (1998).
[10] Wondong Kim, Wookje Kim, S.-J. Oh, J. Seo, J.-S. Kim, H.-G. Min, and S.-C. Hon, Phys. Rev. B **57**, 8823 (1998).
[11] P. Schieffer, C. Krembel, M.-C. Hanf, and G. Gewinner, Phys. Rev. B **55**, 13 884 (1997).
[12] P. Schieffer, C. Krembel, M.-C. Hanf, G. Gewinner, and Y. Gauthier, Phys. Rev. B **62**, 2944 (2000).
[13] P. Schieffer, C. Krembel, M.-C. Hanf, G. Gewinner, and Y. Gauthier, Surf. Rev. Lett. (to be published).
[14] W. Moritz, J. Phys. C **17**, 353 (1984); G. Kleinle, W. Moritz, D. L. Adams, and G. Ertl, Surf. Sci. **219**, L637 (1989); G. Kleinle, W. Moritz, and G. Ertl, *ibid.* **238**, 119 (1990); W. Moritz, H. Over, G. Kleinle, and G. Ertl (unpublished).
[15] J. Philip and J. Rundgren, in *Determination of Surface Structure by LEED*, edited by P. M. Marcus and F. Jona (Plenum, New York, 1984).
[16] J. B. Pendry, J. Phys. C **13**, 937 (1980).
[17] Y. Gauthier, R. Baudoing, Y. Joly, and J. Rundgren, Phys. Rev. B **31**, 6216 (1985).
[18] Y. Gauthier, in *Proceedings of the International Workshop on "Physics and Chemistry of Alloy Surfaces," Dresden, Germany, 1994*, edited by C. Laubschat, K. Muller, and K. Wadelt (World Scientific, Singapore, 1996) [Surf. Rev. Lett. **3**, 1663 (1996)].
[19] P. Schieffer, C. Krembel, M. -C. Hanf, and G. Gewinner, Phys. Rev. B **57**, 1141 (1998).
[20] P. Schieffer, C. Krembel, M. -C. Hanf, M.-H. Tuilier, P. Wetzel, G. Gewinner, and K. Hricovini, Eur. Phys. J. B **8**, 165 (1999).
[21] M. Eder, J. Hafner, and E. G. Moroni, Phys. Rev. B **61**, 11 492 (2000).